Ab initio investigation of the structure and electronic properties of the energetic solids TATB and RDX

A. Barry Kunz
Department of Electrical Engineering, Michigan Technological University, 1400 Townsend Drive, Houghton, Michigan 49931
(Received 4 August 1995)

Solid energetic substances have long played an important technological role as explosives and also as fuels. Much of the research on the solid phases has been concentrated on ground-state properties, and also on the chemistry of the molecules comprising the solid. In addition significant understanding of the detonation properties has been obtained by semiempirical continuum mechanical modeling. Traditional solid-state studies of this important class of materials have mostly been ignored. This may be due to the apparent success of the semiempirical models in describing the detonation properties. Recent interest in more fundamental questions relating to the basic properties of these systems as materials, coupled with a desire to probe fundamental questions relating to the initiation of the chemical reactions leading to combustion/detonation is generating significant interest in the basic solid-state properties of such energetic systems. This interest includes both vibrational and electronic excitations of the solid. The principal concern here is with the electronic states. In this paper, the basic solid-state properties of RDX and TATB are considered. The properties considered include the density and binding energy of the solid, the electronic density of states, and the x-ray structure factors. Computations are performed here at the Hartree-Fock level, using two methods, the LOPAS model developed in our laboratory, and CRYSTAL92.

I. INTRODUCTION

There has been a significant history of interest in the properties of energetic systems undergoing combustion, or detonation. Such systems include solids, liquids, and gases. In this paper, the studies are limited to solid phase systems, and principally consider the electronic properties. Most of the understanding has been obtained using semiempirical continuum models. In addition most of the nonempirical modeling has been focused on properties of the molecule in question, generally in ground-state configurations. This lack of fundamental quantum-mechanical studies is easily understood when one recognizes that mankind has been successfully constructing explosive and pyrotechnic devices for many centuries before the technological methodology needed to understand such systems would be available. In addition, there is a second, and equally serious problem. This is the limitations placed upon such studies by available computational machinery, coupled with the complexity of most useful energetic solids. Solids RDX, $C_3H_6N_6O_6$ (cyclotrimethylene trinitramine), and TATB, $C_6H_6N_6O_6$ (1,3,5 triamino-2,4,6 trinitro-benzene) are considered in this paper. As an illustration of the complexity, consider the following data pertaining to the computations. RDX forms in the *Pbca* lattice structure, and contains 8 RDX molecules in a unit cell.[1] Thus the unit cell contains a total of 168 atoms, and this unit cell possesses a total of 912 electrons, of which only 240 are core electrons. A split valence basis set, as used here consists of 1176 atomic orbitals. TATB is a bit simpler, in that it forms in the $P1$ structure, and contains only 48 atoms per unit cell.[2] Certainly, by traditional solid-state standards, this is still a formidable number of atoms in a cell. This cell contains a total of 264 electrons, of which 72 are core electrons, and a split valence set contains 348 atomic orbitals.

It is a long held belief that initiation (of combustion or detonation) in energetic solids is associated with small regions of the solid termed ''hot spots.''[3,4] The evidence for the existence of these regions is appealing, although circumstantial. However, an atomistic description of what constitutes a ''hot spot'' is not generally agreed upon. In the laboratory, initiation may be accomplished by impacting a pellet of the energetic solid with a hard, massive flyer plate. It is generally seen that the mechanical energy needed to initiate reaction is significantly less than the thermal energy needed for initiation; hence the hypothesis of hot spots.[5,6]

Additional insight is provided by the fractoemission experiments of Dickenson.[7] This series of studies indicates that upon fracture, an energetic solid exhibits substantial charge separation on the fracture surfaces. This is seen to occur even for microcracks, and is concurrent with the emission of energetic particles (electrons, ions), and phonons, or photons from such cracks. This phenomenon may also be related to the nature of the hot spot.

This is in reasonable accord with the theoretical predictions of Coffey.[8] Coffey argues that hot spots in crystals are associated with regions of high shear stress. Normally such regions occur at the surface of the sample, but may be internally generated as well. Such regions are normally accompanied by a high density of dislocations. The Coffey model is far less specific in providing the precise physical effect of such regions on the molecules constituting the solid. In addition to the incompleteness of the Coffey model, this theory does not provide a convincing model for the presence of the charges found in the fractoemission from energetics. Additionally, some studies performed by Kunz and Beck[9] provide strong evidence that the presence of charges inside an energetic solid can provide significant diminution of the strength of molecular bonds, and in some instances even cause their dissociation. Here again the source of the charges is left un-

identified. More recently still, Sanche[10] has provided a model for the aging of dielectric materials caused by free electrons in the conduction band being accelerated by the presence of polar defects in the solid. These systems seem unrelated to the energetics, but upon further investigation, this is not the case. Many dielectric insulators of interest are polymer or molecular solids. In other areas, the utility of conduction electrons in producing radiation damage is also recognized.[11] Here again the source of the electrons is either not described, or is obtained from mechanisms not appropriate to the energetic solids.

Gilman has recently subjected the question of shock sensitivity and initiation in energetic solids to scrutiny, and observes a number of significant factors indicating that excited electronic states play a role in such phenomena.[12] Gilman observes the following: (1) Traditionally, the shock velocity associated with detonation is about 7 km/s (0.7×10^{14} Å/s); (2) the shock fronts are sharp (5 Å); (3) the rise times are short (70 fs); (4) the lattice planes at the front are highly compressed (50%); (5) the fronts are optically opaque; (6) there are very high peak pressures at the shock front (Mbar range); (7) the front is far from thermodynamic equilibrium. This set of observations is used to indicate that mechanisms which require the transport of solid defects are incompatible with the observed shock velocities. This shock velocity is also not compatible with ground-state thermal chemical models involving phonons/vibrons on similar grounds. Gilman argues that shock initiation is related to the metallization of the solid and that sensitivity correlates with the formation of delocalized electrons.

In this paper, an attempt is made to initiate a process of the detailed understanding of the solid-state properties of some energetic materials. This is in hope of eventually developing a fundamental understanding, by which conduction electrons might be generated, as well as a model for the resulting solid-state chemistry. Previously, the author and coworkers have seen that simplifications are sometimes possible in studies of certain properties of energetics, by use of the method of local orbitals.[13] This was demonstrated by a series of studies related to the edge dislocation in RDX.[14] The local orbitals method does provide significant computational benefits in these complex systems, and has been developed into a (sort of) user friendly, automated computer code called LOPAS. This code which stresses local properties is directly able to compute properties such as density and binding energies,[15] but is not able to trivially cope with extensive quantities such as the electron energy band structure. LOPAS includes correlation effects directly by means of many-body perturbation theory (MBPT). An alternate approach is that of direct application of solid-state energy band theory. In the Hartree-Fock (HF) theory used here this is most conveniently done for such systems by use of CRYSTAL92.[16] For part of this work, both methods are employed and the results are found to be in good agreement. Calculations here include crystal density, crystal binding energy, x-ray structure factors, energy bands, and electronic density of states. Studies are performed with a wide variety of basis sets to determine the sensitivity of results to computational details.

The methods used receive a brief description in the next section. This is followed by a more lengthy section detailing the specific results for RDX and TATB. Finally a series of conclusions are drawn from these studies, and some hypotheses are formed as to how these results relate to current thinking on the initiation process.

II. METHODOLOGY

The methods of computation used here are based upon the normal nonrelativistic Hartree-Fock approximation. The use of a nonrelativistic formulation is quite justified for these energetic systems due to the low atomic number of the constituent atoms, the heaviest being O ($Z=8$). In such a case, making the Born-Oppenheimer approximation, the total system Hamiltonian is

$$H=-\frac{\hbar^2}{2m}\sum_{i=1}^{n}\nabla^2-\sum_{i=1}^{n}\sum_{I=1}^{N}\frac{e^2Z_I}{|\mathbf{r}_i-\mathbf{R}_I|}+\frac{1}{2}\sum_{i=1}^{n}\sum_{j=1}^{n}{}'\frac{e^2}{|\mathbf{r}_i-\mathbf{r}_j|}+V_{NN}. \tag{1}$$

Ideally, one would like to solve the time-independent Schrödinger equation for this Hamiltonian,

$$H\Psi_i=E_i\Psi_i. \tag{2}$$

However, for a system containing n electrons and N nuclei, such an exact solution remains impossible, at least for cases of n above 10. In this system the ith electron has a position given by $\mathbf{r}_i$, where spin degrees of freedom are included as needed. Here, $\mathbf{R}_I$ designates the position of the Ith nucleus and its atomic number is Z_I and V_{NN} represents the nuclear repulsion energy. The electron has a charge magnitude e and its mass is m. All calculations are performed using the atomic system of units, for which $e=m=\hbar=1$.

The HF approximation consists of approximating Ψ_i by an antisymmetrized product of one-electron orbitals, $\psi_j(\mathbf{r}_j)$:

$$\Psi_i(\mathbf{r}_1,\ldots,\mathbf{r}_n)\approx\tilde{A}\prod_{j=1}^{n}\psi_j(\mathbf{r}_j). \tag{3}$$

If the one-electron orbitals are chosen variationally, that is, minimizing the expectation value of the Hamiltonian with respect to the assumed form of the wave function, the one-electron orbitals are defined by the HF equation,

$$F(\rho)\psi_i(\mathbf{r}_i)=\varepsilon_i\psi_i(\mathbf{r}_i),$$

$$\rho(\mathbf{r}_1,\mathbf{r}_2)=\sum_{i\leqslant n}\psi_i(\mathbf{r}_1)\psi_i^{+}(\mathbf{r}_2),$$

$$F(\rho)=-\frac{\hbar^2}{2m}\nabla^2-\sum_{I=1}^{N}\frac{e^2Z_I}{|\mathbf{r}-\mathbf{R}_I|}+e^2\int\frac{\rho(\mathbf{r}_2,\mathbf{r}_2)}{|\mathbf{r}-\mathbf{r}_2|}\,d\mathbf{r}_2-e^2\frac{\rho(\mathbf{r},\mathbf{r}_2)}{|\mathbf{r}-\mathbf{r}_2|}\hat{P}(\mathbf{r}_2,\mathbf{r}), \tag{4}$$

where $\hat{P}$ is the operator that interchanges the designated coordinates. This is the system of equations which is termed the canonical HF equations, and is the system solved by matrix techniques for the infinite, pure, perfect, periodic lattice problem (the band structure problem) by the code CRYSTAL92. The discussion of the choice of basis set is deferred until later. An excellent, basic discussion of the flex-

ibility allowed by the HF type problem is provided by Gilbert,[17] who also indicates systematic ways to exploit this flexibility.

An alternate approach, normally used by the author's research group and his associates, to perform studies on defects in solids, is based upon the local orbitals approach of Kunz and Klein.[18] This approach is also valid for the band-structure problem.[19] In the case of energetic solids where the unit cell consists of multiple identical chemical building blocks, this approach is attractive in terms of efficiency. Here, for example, RDX solid has a unit cell consisting of eight identical RDX formula units, $C_3H_6N_6O_6$. This approach allows one to simply describe only one of these formula units and obtain the cell description by symmetry operations. The case of TATB is less attractive, in that the TATB unit cell has only two identical formula units.

The local orbitals equation is obtained by performing a canonical transformation on the HF problem. This is done by using the arbitrary localization operator W chosen to interrupt the lattice periodicity, and permits solutions to the resulting equations which decay with distance. The canonical HF solutions do not decay but rather obey periodic boundary (Bloch) conditions. This procedure requires that the following set of equations be solved:

$$[F_A+U_A+\rho W\rho]\phi_i=\hat{\varepsilon}_i\phi_i\,,$$

$$U_A=V_A^S+V_A^{\mathrm{PI}}\,,$$

$$W=-V_A^S\,,$$

$$[F_A+V_A^{\mathrm{PI}}+V_A^S-\rho V_A^S\rho]\phi_i=\hat{\varepsilon}_i\phi_i\,. \tag{5}$$

Here the definition of ρ remains unchanged except that one uses the solutions to Eq. (5) to form ρ rather than those of Eq. (4).

Additionally, one chooses F_A to represent the HF operator for the Ath formula unit in the lattice. In the present case this is either an RDX or a TATB unit. The remainder of the HF operator is contained in U_A. This is traditionally further broken into a long-range, or point ion part V_A^{PI} (which in the present cases is identically zero) and a short-range remainder V_A^S. This then defines the local orbital problem at the HF level. The complexity of the present problems dictates that these studies be performed at this level currently, and the inclusion of explicit correlation is possible but prohibitively expensive at this time.

III. COMPUTATIONAL RESULTS

Both codes employed in this study expand the one-electron orbitals in a series of contracted Cartesian Gaussian orbitals. This is currently a standard approach to molecular and solid-state problems. CRYSTAL92 has preprogrammed in it several possible sets of Gaussian functions using the Pople scheme.[16] These sets include STO-ng sets, where STO is Slater-type orbital and n is a number parameter chosen by the user; also CRYSTAL92 includes the possibility of both 3-21g and 6-21g split valence sets as well. Finally, it is possible to employ general and arbitrary basis sets as long as no higher angular momentum states than d-like are used. One final degree of freedom is that the standard sets may be scaled in range from the Pople norm, this feature being quite useful in the present studies, as the outer (most diffuse) Gaussian basis vector provided by the Pople prescription is frequently too diffuse to be optimal in these solid-state calculations. In the present cases, variationally better solutions are normally found by scaling the outer Gaussian to shorter range, which also minimizes linear dependence effects as well. The LOPAS code offers other orbital choices, normally based upon the sets produced by Huzinaga.[20] The smallest sets are essentially STO-3g sets using different Gaussian exponents for the 2s and 2p sets. The intermediate choice is a double-ζ basis set, and the largest provided is a double-ζ plus polarization function set. In addition, it is possible to use general basis sets as in the CRYSTAL92 case; however LOPAS permits the inclusion of f-type orbitals. It would be desirable from the standpoint of computational efficiency to use small STO-ng sets, if the accuracy is not compromised by such sets.

Studies of the sensitivity of results to basis set were conducted primarily with the CRYSTAL92 code. This was done for the TATB system. To perform these studies the structure of the TATB molecule as determined experimentally was used initially. This molecule was placed in the experimentally determined $P1$ geometry. The ratios of the lengths of the three lattice vectors were taken from experiment, as were the experimental angles. The basic cell volume was varied. This is equivalent to studying TATB under hydrostatic compression. These studies include a rather crude STO-2g set, a more standard STO-3g set, and finally a 6-21g set. In the latter case the outer exponent was scaled on each atom to obtain a ''best'' energy variationally. This produced a scaling factor of 1.05 for hydrogen and 1.10 for the three heavy atoms (C,N,O). All 6-21g results quoted here are for this scaling. The basic parameter of merit here is the predicted crystal density. Experimentally, the density of TATB is about 1.94 g/cm^3. Using the optimal STO-2g solution a density prediction of 1.67 g/cm^3 (14% error) is obtained. Using the more accurate STO-3g set the density prediction improves to 1.73 g/cm^3 (11% error). Finally, using the optimal 6-21g basis set the density prediction improves to a value of 1.89 g/cm^3 (2.5% error). This later value seems to be in reasonable accord with experiment, and certainly establishes the 6-21g basis set as the preferred one, despite the significant incremental cost.

The result for TATB was subjected to the further test of being compared to the LOPAS results. The LOPAS calculation was performed using a double-ζ accuracy basis set. This corresponds reasonably to the 6-21g set used above, although it is a bit more accurate. Again the TATB molecular geometry was taken from experiment. The crystal was again formed in the $P1$ geometry; however, the three defining lattice vector lengths were varied independently, as were the three crystal angles. The angles were computed to be within 1° of experiment, and for later work the experimental angles are used. The A vector had a length slightly longer (1%) than that found in CRYSTAL92, the B vector had a length identical to that found by CRYSTAL92, and the length of the C vector was slightly shorter than that predicted by CRYSTAL92 (again 1%). The final density predicted by LOPAS is therefore also 1.89 g/cm^3.The agreement between the codes in this case is quite fine. Since most parameters of further interest to this study

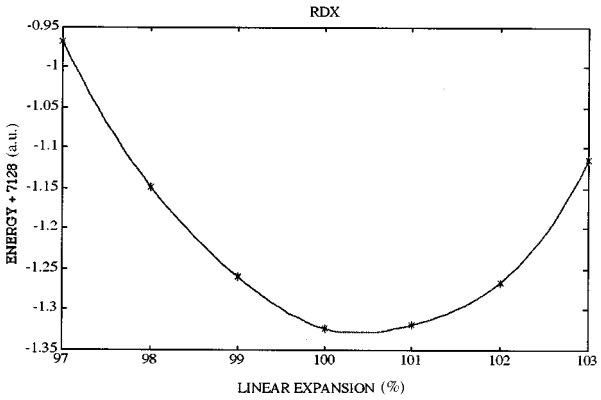

FIG. 1. The binding energy is shown, for RDX solid, in a hydrostatic compression mode. The compression is for a linear dimension and is shown as a percent of the experimentally determined distance. Energies are per unit cell and are in a.u. An amount of 7128 a.u. has been added to the energy.

refer to the extended crystal, the results of CRYSTAL92 are taken, as for such studies this is more convenient. In addition all results, whether for TATB or RDX, are obtained using the optimized 6-21*g* basis set described earlier.

RDX is one of the standard energetic solids in current use. It is reasonably sensitive to detonation, when subjected to standard drop-hammer tests, but not so sensitive as to preclude practical usage.[21,22] Experimentally, RDX forms in a *Pbca* structure, The lengths of the three crystalline lattice vectors are 13.192 Å, 11.574 Å, and 10.709 Å, respectively, as is appropriate to the *Pbca* structure the crystalline angles are all 90°.[1] Using CRYSTAL92 and the experimental atom coordinates for the RDX molecule, the lattice vector lengths were varied in a hydrostatic manner to obtain an energy minimum. The binding energy curve for this hydrostatic distortion mode is seen in Fig. 1. It is clear from this figure that an energy minimum is achieved for a linear dimension that is 100.2% of the experimental value. This corresponds to a crystal density that is 1.79 g/cm^3, a value in good agreement with the experimental value of 1.80 g/cm^3.

The theoretically determined geometry was used for all further calculations, although in this case the differences are not significant. The crystal binding energy was computed and it is found that the RDX solid is stable against decomposition into atoms by 8.9416 a.u. (243.21 eV) per unit cell, or about 0.053 22 a.u./atom (1.45 eV/atom). Although there is little to actually compare this value with, the strength seems in keeping with values to be expected from other HF determinations of covalent bond strengths for similar quality basis sets.

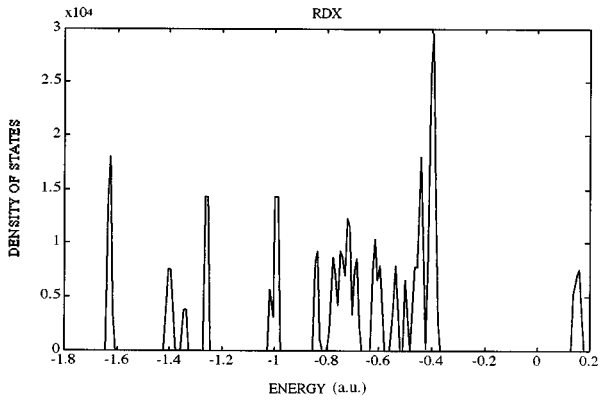

FIG. 2. The total electronic density of states is given for solid RDX. The density of states is in states/a.u., and the unit of energy is the a.u. Negative energy states are occupied.

TABLE I. The x-ray structure factors are given for solid RDX. The factors h, k, and l are integers multiplying the primitive lattice vectors in the reciprocal lattice and identify the specific structure factor. Computations of both real and imaginary parts of the structure factors were performed, but as expected, the imaginary parts were essentially zero ($<10^{-13}$). A more complete list of structure factors will be provided by the author upon request.

h	k	l	Real part of structure factor
0	0	0	912.0
1	0	0	0.000
2	0	0	102.0
3	0	0	0.000
2	1	0	−85.11
0	2	0	36.38
2	2	0	−138.3
2	3	0	−19.24
1	1	1	68.08
2	1	1	31.37
3	1	1	−17.11
0	2	1	117.2
1	2	1	−12.37
2	2	1	96.15
3	2	1	−50.32
1	3	1	−122.9
2	3	1	−4.510
3	3	1	−39.74
0	0	2	−93.32
1	0	2	148.5
2	0	2	40.98
3	0	2	−34.32
1	1	2	−13.82
2	1	2	−22.59
3	1	2	−55.99
0	2	2	−60.08
1	2	2	44.05
2	2	2	11.98

The energy band structure was computed for the RDX crystal; however since there are some 672 valence electrons per unit cell, corresponding to some 336 energy bands, when spin degeneracy is taken into account, little is learned from actually viewing the energy band diagram. What is more useful however is the determination of the electronic density of states, or the number of energy levels lying in a region of energy between E and $E+dE$. This is seen for RDX in Fig. 2. The energy levels lying below the zero of energy are all occupied levels, whereas those lying above the zero of energy correspond to virtual (conduction) levels. Clearly from this energy diagram RDX is a wide-gap insulator. However in the absence of computed correlation corrections an accu-

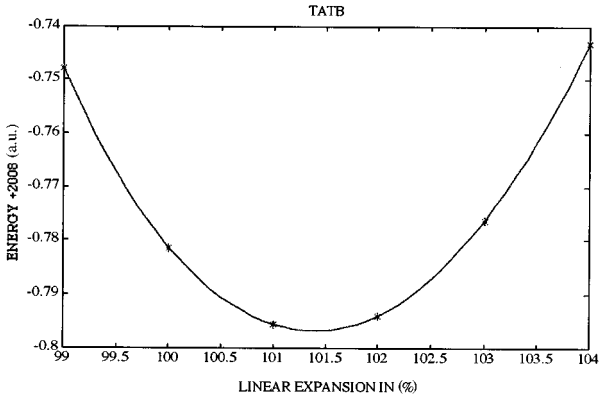

FIG. 3. The binding energy is shown, for TATB solid, in a hydrostatic compression mode. The compression is for a linear dimension and is shown as a percent of the experimentally determined distance. Energies are per unit cell and are in a.u. An amount of 2008 a.u. has been added to the energy.

rate estimate of the band gap is not possible at this time. Finally the x-ray structure factors have been computed for RDX crystal. The first few of these are seen in Table I.

Similar results are available for the TATB system. TATB is also a current practical energetic material. It differs from systems such as RDX most notably in that it is highly insensitive to detonation. In fact, in terms of the drop-hammer-type test, it is one of the most if not the most insensitive explosive in current use. The hydrostatic binding curve is seen in Fig. 3. TATB is found to be bound by 4.372 61 a.u. (118.935 eV) per unit cell. This translates to a binding of about 0.0911 a.u./atom (2.478 eV/atom). The band structure was computed for TATB as well, and the electronic density of states is shown in Fig. 4. Here as for RDX the levels below the zero of energy represent occupied valence levels, and those above the zero represent virtual levels. Again the system is a wide gap insulator, and again, absent a correlation calculation, the exact theoretical gap is not available. Finally, the first few x-ray structure factors are seen in Table II. A discussion of the possible significance in the differing electronic densities of states is found in the conclusions.

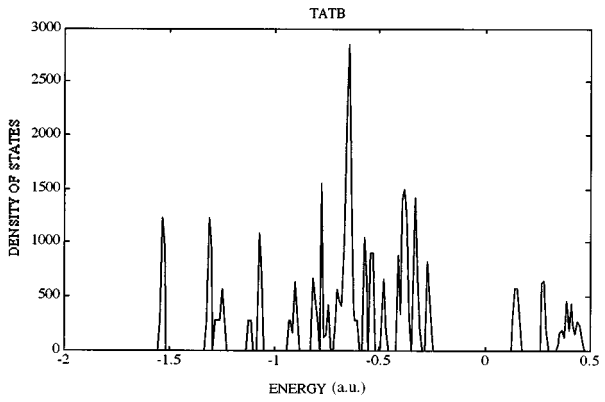

FIG. 4. The total electronic density of states is given for solid TATB. The density of states is in states/a.u., and the unit of energy is the a.u. Negative energy states are occupied.

TABLE II. Sample x-ray structure factors are given for solid TATB. The factors h, k, and l are integers multiplying the primitive lattice vectors in the reciprocal lattice and identify the specific structure factor. Computations of both real and imaginary parts of the structure factors were performed, but as expected, the imaginary parts were essentially zero ($<10^{-13}$). A more complete list of structure factors will be provided by the author upon request.

h	k	l	Real part of structure factor
0	0	0	264.0
1	0	0	−19.53
2	0	0	−0.3980
3	0	0	20.02
4	0	0	2.109
5	0	0	−13.05
0	1	0	13.01
1	1	0	37.57
2	1	0	−10.15
3	1	0	17.00
4	1	0	−6.426
5	1	0	−5.403
0	2	0	1.755
1	2	0	−25.32
2	2	0	−84.02
3	2	0	14.01
4	2	0	5.212
5	2	0	−1.234
0	3	0	−24.52
1	3	0	−15.86
2	3	0	−6.211
3	3	0	−20.51
4	3	0	7.825
5	3	0	2.301
0	4	0	−0.8848
0	0	1	−3.550
1	0	1	−20.24
1	1	1	18.69

IV. CONCLUSIONS

There are several simple conclusions that may be drawn immediately. First, it is clearly possible to use the HF model to perform density predictions on this rather complicated class of molecular solids. The computational effort is not unreasonably extreme. The present calculations were all performed using a Digital Equipment Corp. Alpha scientific workstation model 3000-500x. This system is equipped with 256 megabytes of main memory, and about 8 gigabytes of disk space. For the computations performed in this particular study, the available amounts of main memory and disk space were not required; however for more complex energetic solids under current study, these resources are useful. Computer speed is also adequate for these studies. A single, complete, self-consistent study of a given geometry and set of lattice vector lengths is accomplished in a few hours to at most 1 day, depending upon the exact situation.

We have also seen at the HF level of computation that both the LOPAS and the CRYSTAL92 model are able to produce similar results. This provides additional verification of the

reliability of either computation for these solids, and a heightened sense of comfort with the results obtained. The binding energies have been obtained in the HF limit for both systems, and the more sensitive RDX crystal is found to have an average binding of 1.45 eV/atom, whereas the far less sensitive TATB was found to have an average binding of 2.48 eV/atom. Clearly these binding energies would increase with the inclusion of correlation corrections; however, the obtained differences in binding energies are significantly large that correlation corrections are not seen as likely to negate the qualitative nature of this result.

The stability here is quoted with respect to decomposition into atoms. This is a bit unusual in that it might be expected to consider decomposition into the molecular formula units. However, in the case of energetic systems this is not a useful measure. The isolated individual molecule of RDX or TATB is not the usual state for decomposition in that this molecular state is only metastable. The decomposition is net exothermic, and the final decomposition products are a blend of molecular species that are beyond the scope of this work. Therefore the atom state is used as the energy zero here. It has the virtue of being well defined, and an interested party can compute from these data energetic properties of various decomposition paths as needed. What is clear from these results is that in terms of overall energetic stability, TATB is more stable than is RDX.

We have also seen that some additional traditional solid-state-type of properties have been possible to evaluate, including band structure, electronic density of states, and x-ray structure factors. It is also possible to deduce some additional useful data from the results obtained. For example, the bulk modulus B may be computed for the hydrostatic compression mode used for geometric optimization:

$$B=\left(V \frac{d^2U}{dV^2} \right)_{V_0} . \tag{6}$$

For this deformation, B is found to be 37.0 GPa for RDX, and 40.6 GPa for TATB.

Finally, we may comment further on some possible differences between RDX and TATB. As mentioned before, RDX is a relatively sensitive explosive, whereas TATB is highly insensitive. Some explanation for this is found in this study. The other parameter seen in this study which is quite different at both a qualitative and quantitative level concerns the electronic density of states. This is most noticeable for the upper portion of the valence density of states. In the case of RDX as seen in Fig. 2 the upper portion contains a significant proportion of the occupied states, whereas for TATB as seen in Fig. 4 this upper portion has relatively few states. Typically the valence states in an energetic solid are the bonding orbitals. In RDX there is a very substantial number of these bonding orbitals with energy at the top of the valence structure, whereas for TATB the peak number of bonding orbitals are well buried in the valence structure. At the top of the TATB valence bands, one finds relatively few states when compared to RDX. This factor, coupled with the binding energy per atom, may well be consistent with the high stability noted for TATB, as well as its lower energy output. Explicit modeling of decomposition models is under way, and will be the topic of future work.

ACKNOWLEDGMENTS

The author wishes to express his appreciation to Dr. Richard S. Miller for support of this research, and to Dr. Herman Ammon, of the University of Maryland, and Dr. Alan Pinkerton, of the University of Toledo, for their advice and encouragement. Research supported in part by the U.S. Navy, Office of Naval Research under Grant No. N00014-91-J-1953.

[1] C. S. Choi and E. Prince, Acta Crystallogr. Sect. B **28**, 2857 (1972).
[2] J. Sharma and B. C. Beard, in *Structure and Properties of Energetic Materials*, edited by D. H. Liebenberg, R. W. Armstrong, and J. J. Gilman, MRS Symposia Proceedings No. 296 (Materials Research Society, Pittsburgh, 1993), p. 189.
[3] R. D. Bardo, in *Shock Waves in Condensed Matter*, edited by Y. M. Gupta (Plenum, New York, 1985), p. 843.
[4] W. L. Elban, R. G. Rosemeir, K. C. You, and R. W. Armstrong, Chem. Propulsion Inf. Agency **404**, 81 (1984).
[5] G. E. Duval, in *Shock Waves in Condensed Matter* (Ref. 3), p. 1.
[6] J. K. Dienes, Chem. Propulsion Inf. Agency **404**, 19 (1984).
[7] T. Dickenson, Chem. Propulsion Inf. Agency **404**, 153 (1984).
[8] S. F. Coffey, Phys. Rev. B **24**, 6984 (1981).
[9] A. B. Kunz and D. R. Beck, Phys. Rev. B **36**, 7580 (1987).
[10] L. Sanche L, IEEE Trans. Electr. Insulation **28**, 789 (1993).
[11] A. Slugar, J. Phys. C **21**, L431 (1989); A. Slugar and E. Stefanovich, Phys. Rev. B **42**, 9664 (1990).
[12] J. J. Gilman, Chem. Propulsion Inf. Agency **589**, 379 (1992).
[13] A. B. Kunz, Theor. Chim. Acta **84**, 353 (1993).
[14] G. Gao, R. Pandey, and A. B. Kunz, in *Structure and Properties of Energetic Materials* (Ref. 2), p. 149.
[15] A. B. Kunz, J. Phys. Condens. Matter **6**, 1233 (1994).
[16] R. Dovesi, C. Pisani, C. Roetti, M. Causa, and V. R. Saunders, CRYSTAL88, Quantum Chemistry Program Exchange, Program No. 577 (Indiana University, Bloomington, IN, 1989); R. Dovesi, V. R. Saunders, and C. Roetti, CRYSTAL92 User Documentation, University of Torino, Torino, and SERC Daresbury Laboratory, Daresbury, UK, 1992.
[17] T. L. Gilbert, in *Molecular Orbitals in Chemistry, Physics, and Biology*, edited by P. O. Lowdin and B. Pullman (Academic, New York, 1964), p. 405.
[18] A. B. Kunz and D. L. Klein, Phys. Rev. B **17**, 4614 (1978).
[19] A. B. Kunz, Phys. Rev. B **26**, 2056 (1982).
[20] S. Huzinaga, *Gaussian Basis Sets for Molecular Calculations* (Elsevier, Amsterdam, 1984).
[21] M. Von Thiel, F. H. Ree, and J. Sayer, in *Shock Waves in Condensed Matter* (Ref. 3), p. 883.
[22] M. F. Folz and A. L. Nichols III, Chem. Propulsion Inf. Agency **589**, 299 (1992).